On the extension of LES methods from incompressible to compressible turbulent flows with application to turbulent channel flow.

J B Pedro[1] [2], A Bàez Vidal[1], O Lehmkuhl[1], C D Pérez Segarra[1] and A Oliva[1]

[1] Heat and Mass Transfer Technological Centre (CTTC), Universitat Politècnica de Catalunya - BarcelonaTech (UPC), ESEIAAT, Carrer Colom 11, 08222 Terrassa (Barcelona), Spain.
[2] Termo Fluids S.L., Avinguda Jaquard, 97 1-E, 08222 Terrassa (Barcelona), Spain.

E-mail: juan@cttc.upc.edu

Abstract. The objective of the present work is to validate the compressible Large-Eddy Simulation (LES) models implemented in the in house parallel unstructured CFD code TermoFluids. Our research team has implemented and tested several LES models over the past years for the incompressible regimen. In order to be able to solve complex turbulent compressible flows, the models are revisited and modified if necessary. In addition, the performance of the implemented hybrid advection scheme is an issue of interest for the numerical simulation of turbulent compressible flows. The models are tested in the well known turbulent channel flow problem at different compressible regimens.

1. Introduction

The aim of this work is to validate the compressible extension of the existing incompressible Smagorinsky (SMG), Wall-Adaptive Large-Eddy (WALE) and Variational Multiscale (VMS) turbulence models implemented in the in-house software TermoFluids [1]. This models have been tested in several cases, such as the flow over a NACA0012 airfoil [2] [3] and a circular cylinder [4]. The compressible solver implemented in TermoFluids uses a kinetic-energy preserving second-order spatial scheme, carefully hybridized with a low-order dissipative upwind scheme in order to stabilize the method in the presence of flow discontinuities. Our objective is to study the performance of the LES methods, along with the hybrid advection scheme, in the turbulent channel flow in order to validate them and then explore its application in more complex problems, such as turbulent flows with SBLIs.

Direct numerical simulation (DNS) has the advantage of resolving all scales of fluid motion, but its high computational requirements restirct its use for the study of simplified problems, specially for high-speed and high-Reynolds flows. The Reynolds Averaged Navier Stokes (RANS) approach has been widely used to overcome DNS restrictions. It allows less expensive simulations, since turbulence is not directly resolved, introducing the need of turbulence modeling [5]. However, the time averaging procedure leads to extra correlations that appear throughout the equations of motion, and turbulence modeling must close these new unknowns [6]. The extension of the RANS methods to the compressible solver was already examined in previous works [7], concluding that such approach may lead to unsatisfactory predictions

of flows with significant SBLI. Discrepancies can be attributed to various deficiencies in the models, such as a failure to resolve anisotropy of the normal stresses. It is also a concern that steady state solvers will be in error if the flow is naturally unsteady and the shock location oscillates. On the other hand, LES solve the largest scales of motion and model the smallest non-resolved scales, resulting in a less-demanding approach than DNS that can overcome the inherent problems of the RANS approach (but at higher computational cost). Hence, LES seems to be perfect candidate to carry out computations of high-Reynolds, high-speed turbulent flows. LES have been extensively developed for incompressible flows, and the compressible approach usually consists of an extension of existing models [8]. LES has not been widely applied to shock/boundary-layer interaction problems [9], so its performance is an issue of increasing interest. We explore in this work the ability of the LES models to deal with compressible turbulent flows in different compressible regimens. To that purpose, the well known turbulent channel flow is simulated with the aforementioned turbulence models and compared with reference DNS and experimental data.

The first DNS of incompressible turbulent plane channel flow was performed by Kim et al. [10], used to compare nearly incompressible results (here referred as KIM). The Reynolds number based on friction velocity was around 180 ($Re_\tau \approx 180$). A large number of turbulence statistics including turbulence intensities, Reynolds shear stress, vorticity, high order statistics, etc., were compared with experimental data with good agreement.

DNS of turbulent compressible supersonic channel flow between isothermal walls was performed by Coleman et al. [11] (here referred as COL). The Mach numbers based on the bulk velocity and sound speed at the walls were 1.5 (used for the supersonic results comparison) and 3. The Reynolds numbers were 3000 ($Re_\tau \approx 222$) and 4880 ($Re_\tau \approx 451$) respectively, based on the bulk velocity and channel half-width. They found that the mean density and temperature gradients caused enhanced streamwise coherence of near-wall streaks. Other works exist focused on the study of compressiblity effects and turbulence scaling in turbulent supersonic channel flow with isothermal walls, such as Foysi et al. [12] (here referred as FOY).

2. Numerical Model

2.1. Favre-averaged Navier-Stokes Equations

In LES the contribution of the large, energy-carrying structures to momentum and energy transfer is computed exactly and only the effect of the smallest scales of turbulence is modeled. While a substantial amount of research has been carried out into modeling for the LES of incompressible flows, applications to compressible flows have been significantly fewer, due to the increased complexity introduced by the need to solve an energy equation, which introduces extra unclosed terms. Furthermore, the form of the unclosed terms depends on the chosen energy equation [13]. To obtain the equations governing the motion of the resolved eddies, we must separate the large from the small scales. LES is based on the definition of a spatial filter operator:

$$\overline{f}(x) = \int_D f(x')G(x, x'; \overline{\Delta})dx' \tag{1}$$

where D is the entire domain, G is the filter function, and $\overline{\Delta}$ is the filter-width associated with the wavelength of the smallest scale retained by the filtering operation. Thus, the filter function determines the size and structure of the solved scales. In compressible flows it is convenient to use Favre-filtering to avoid the introduction of SGS terms in the equation of conservation of mass. Applying the Favre-filtering operation to the Navier-Stokes (NS) equations, we obtain the following system of equations:

$$\overline{\rho}_t + \nabla \cdot (\overline{\rho}\tilde{\mathbf{u}}) = 0 \tag{2}$$

$$(\overline{\rho}\tilde{\mathbf{u}})_t + \nabla\cdot(\overline{\rho}\tilde{\mathbf{u}}\tilde{\mathbf{u}}) = \nabla\cdot(\overline{\tau} - \overline{\rho\mathbf{u}''\mathbf{u}''}) - \nabla\overline{p} \tag{3}$$

$$\overline{E}_t + \nabla\cdot(\overline{H}\tilde{\mathbf{u}}) = \nabla\cdot(\tilde{\mathbf{u}}(\overline{\tau} - \overline{\rho\mathbf{u}''\mathbf{u}''})) - \nabla\cdot(\overline{\mathbf{q}} + \overline{\mathbf{u}''H''} - \overline{\tau\mathbf{u}''} + \overline{\rho\mathbf{u}''k}) \tag{4}$$

where $\overline{\phi}$ refers to the mean value in time of the varibale ϕ and $\tilde{\phi} = \overline{\rho\phi}/\overline{\rho}$ is its Favre average. ρ is the fluid density, $\mathbf{u} = (u_1, u_2, u_3)$ is the velocity vector referred to the coordinate system $\mathbf{x} = (x_1, x_2, x_3)$, p is the pressure, and E is the total energy. The subscript $(\cdot)_t$ refers to the time derivative $\partial/\partial t$. The fluid total enthalpy is $H = E + p$. The viscous stress tensor is defined as,

$$\tau_{ij} = 2\mu(S_{ij} - \frac{1}{3}S_{kk}\delta_{ij}) \tag{5}$$

where μ is the fluid viscosity and $S_{ij} = \frac{1}{2}(\frac{\partial u_i}{\partial x_j} + \frac{\partial u_j}{\partial x_i})$. Finally, $\mathbf{q} = -\kappa\nabla T$ is the heat flux, where $\kappa = \frac{\mu c_p}{Pr}$ and T is the temperature. In the present study the working fluid is air with the ideal gas hypothesis, with $\gamma = 1.4$, $c_p = 1004\ \ [Jkg^{-1}K^{-1}]$, and $Pr = 0.72$.

$$E = \frac{p}{\gamma - 1} + \frac{1}{2}\rho\mathbf{u}\cdot\mathbf{u} \tag{6}$$

The system of equations is closed with the equation of state,

$$\overline{p} = \overline{\rho}R\tilde{T} \tag{7}$$

being $R = 287\ \ [Jkg^{-1}K^{-1}]$. The viscosity is computed with the Sutherland's law,

$$\mu = 1.461^{-6}\frac{T^{3/2}}{110.3 + T} \tag{8}$$

Equations (2) (3) and (7) differ form their laminar counterpart only by the appearance of the Favre-averaged Reynolds-stress tensor, $\tau_T = -\overline{\rho\mathbf{u}''\mathbf{u}''}$. Several terms appear in equation (4), the turbulent transport of heat $\mathbf{q}_T = \overline{\mathbf{u}''H''}$, the molecular diffusion $\overline{\tau\mathbf{u}''}$ and the turbulent transport of turbulent kinetic energy $\overline{\rho\mathbf{u}''k}$. The definition of the total energy is also modified, $\overline{E} = \frac{\overline{p}}{\gamma-1} + \frac{1}{2}\overline{\rho}\tilde{\mathbf{u}}\tilde{\mathbf{u}} + \overline{\rho k}$.

The closure approximations used in the present study are [5]:

$$\tau_T = 2\mu_T(\tilde{S}_{ij} - \frac{1}{3}\tilde{S}_{kk}\delta_{ij}) - \frac{2}{3}\overline{\rho}k^{SGS}\delta ij \tag{9}$$

$$\mathbf{q}_T = -\frac{\mu_T c_p}{Pr_T}\nabla\tilde{T} \tag{10}$$

Where μ_T and k^{SGS} depend on the subgrid model (see Secs. 2.3 to 2.5). $Pr_T = 0.6$ is the turbulent Prandtl number The molecular diffusion and the turbulent transport of turbulent energy are approximated together as follows:

$$\overline{\tau\mathbf{u}''} - \overline{\rho\mathbf{u}''k} = (\mu + \frac{\mu_T}{\sigma_k})\nabla k \tag{11}$$

Although this term is only relevant for hypersonic flows, where σ_k is a constant. The problem reduces, therefore, to the computation of the eddy viscosity μ_T.

2.2. Numerical schemes

TermoFluids is a unstructured parallel finite volume solver. After discretization of the computational domain in a finite number of control volumes, NS equations are solved for each volume,

$$\frac{\partial \phi}{\partial t} = \frac{1}{V_c} \sum_f f(\phi_f) \mathbf{n} A_f \tag{12}$$

Where $\phi = (\rho, \rho\mathbf{u}, E)$ contains the conserved variables, V_c is the volume of the finite volume, $\mathbf{n}$ is the face normal vector corresponding to the face with surface A_f and with flux $f(\phi_f)$, where ϕ_f is the variable vector at the face and depends on the numerical scheme. A hybrid advection numerical scheme is used for the discretization of the convective flux. The scheme is based on a kinetic-energy preserving numerical scheme, F^{KEP}, that ensures kinetic-energy preserving at all scales, this is important for DNS and LES since numerical diffusion can dissipate the smallest scales altering the result. Convective terms are discretized in split form in order to ensure temporal stability [14]. To avoid instabilities in the presence of shock-waves, a low-order upwind scheme, F^{UP}, is used when a discontinuity in the flow is detected. The shock detection is carried out with a Larsson discontinuity sensor [15].

$$F^{inv}(\phi_f) = (1 - \Phi) F^{KEP}(\phi_f) + \Phi F^{UP}(\phi_f) \tag{13}$$

where Φ stands for the sensor, which only takes values of 0 (smooth flow) or 1 (discontinuity detected).

Viscous terms are discretized with a central-difference approximation and a second-order Adam-Bashford scheme is used for the temporal integration.

2.3. The Smagorinsky model

The compressible version of the Smagorinsky model was proposed in [16],

$$\mu_t = f_{vd} C_R \overline{\rho} \Delta^2 \sqrt{\tilde{S}_{mn} \tilde{S}_{mn}} \tag{14}$$

with $C_R = 0.01$. The SGS isotropic stress tensor term is given by,

$$k^{SGS} = C_I \Delta^2 \tilde{S}_{mn} \tilde{S}_{mn} \tag{15}$$

where $C_I = 0.0066$. The Smagorinsky model is known to fail in the inner portion of the boundary layer, this is why a van Driest damping factor is used.

$$f_{vd} = 1 - e^{(-y^+/26)} \tag{16}$$

2.4. The WALE model

The WALE model by Nicaud and Ducros [17] is based on the square of the velocity gradient tensor. In its formulation the SGS viscosity accounts for the effects of both, the strain and the rotation rate of the smallest resolved turbulent fluctuations. In addition, the proportionality of the eddy viscosity near walls is recovered without any dynamic procedure,

$$\mu_t = \overline{\rho} C_w^2 \Delta^2 \frac{(\tilde{s}_{ij} \tilde{s}_{ij})^{3/2}}{(\tilde{S}_{ij} \tilde{S}_{ij})^{5/2} + (\tilde{s}_{ij} \tilde{s}_{ij})^{5/4}} \tag{17}$$

where $C_w = 0.325$ is a true model constant, $\tilde{S_{ij}}$ is the strain rate tensor of the resolved field and $\tilde{s_{ij}}$ is the traceless symmetric part of the square of the resolved velocity gradient tensor.

$$\tilde{s_{ij}} = \frac{1}{2}\left(\frac{\partial \tilde{u}_i}{\partial x_l}\frac{\partial \tilde{u}_l}{\partial x_j} + \frac{\partial \tilde{u}_j}{\partial x_l}\frac{\partial \tilde{u}_l}{\partial x_i}\right) - \frac{1}{3}\frac{\partial \tilde{u}_m}{\partial x_l}\frac{\partial \tilde{u}_l}{\partial x_m}\delta_{ij} \tag{18}$$

The aforementioned expressions are developed for incompressible flow, and it thus gives only μ_t. The modification is to use the relation between μ_t and k^{SGS} from the original Smagorinsky model in order to close equation (9) in the computation of the isotropic SGS tensor.

$$\tau_T = 2\mu_T(\tilde{S}_{ij} - \frac{1}{3}\tilde{S}_{kk}\delta_{ij}) - \frac{2}{3}\frac{C_I'}{\overline{\rho}}\left(\frac{\mu_t}{\Delta}\right)^2\delta_{ij} \tag{19}$$

where $C_I' = 45.8$. With that we have updated the model to deal with compressible flows.

2.5. The Variational Multiscale model

In the Variational Multiscale approach three classes of scales are considered: large, small and unresolved scales. If a second filter with filter length $\hat{l}$ is introduced (usually called test filter), a splitting of the scales can be performed,

$$f' = \overline{f} - \hat{f} \tag{20}$$

Neglecting the effect of unresolved scales, we only need to model the small scales. Here, we close these terms using the WALE model.

3. Turbulent Channel Flow

3.1. Description of the LES

The channel flow is a good candidate to study wall turbulence because it is homogeneous in two directions, avoiding uncertainties of the boundary conditions. Isothermal walls at $T_w = 500K$ are imposed in the remaining boundaries. The flow is initialized with a Pouseille function that introduces early disturbances to the flow. Once the turbulent state is achieved, average of the flow is computed in order to further evaluate turbulent statistics.

Six different cases were studied at two different compressibility regimens. First, a $M = 0.3$ and $Re = 2820$ (based on the bulk velocity, wall properties and channel semi-height) turbulent channel flow was simulated in order to evaluate the LES models in the near incompressible regimen. Reference results are available for comparison: Kim et al. [10], Foysi et al. [12] and also experimental data can be found for the incompressible channel flow [18]. Afterward, a $M = 1.5$ and $Re = 3000$ channel flow was studied to asses the LES performance in the supersonic regimen. Reference results are available for comparison: Coleman et al. [11] and Foysi et al. [12]. See table (1) for all the details.

In this paper the performance of the LES models on the compressible channel flow are explored with reference to mean profiles and second-order statistics of velocity and thermodynamic properties, compared to reference DNS and experimental data.

3.2. Results

We begin with the analysis of mean flow properties. The time evolution of u_τ for the case M03 is depicted in figure (1) for the different LES models. WALE and VMS models converge well to the DNS average value (marked with solid line), the SMG model over-predicts this value. Figure (2) shows the law of the wall for both cases. Results show good tendency and match reference data except for the SMG model. For the subsonic case, results for the WALE and VMS models match slightly better experimental data by Eckelmann et al. [18] but they also approximate very well to the wall of the law and DNS data. The failure of the SMG model in reproducing flow mean properties is more visible. Results for the supersonic case agree with

Table 1. Data for the different cases.

Case	M	Re	Re_τ	L_x	L_y	L_z	N_x	N_y	N_z	Δx^+	Δy_w^+	Δz^+
M03	0.3	2820	181	12	2	6	64	64	96	19	0.5	6
KIM	0	2300	180	4π	2	2π	192	129	160	12	0.05	7
FOY	0.3	2820	181	9.6	2	6	192	129	160	9.12	1.02	6.84
M15	1.5	3000	221	12	2	6	64	64	96	19	0.5	6
COL	1.5	3000	220	4π	2	$4\pi/3$	114	119	80	19	0.1	12
FOY	1.5	3000	221	4π	2	$4\pi/3$	192	151	128	14.46	0.84	7.23

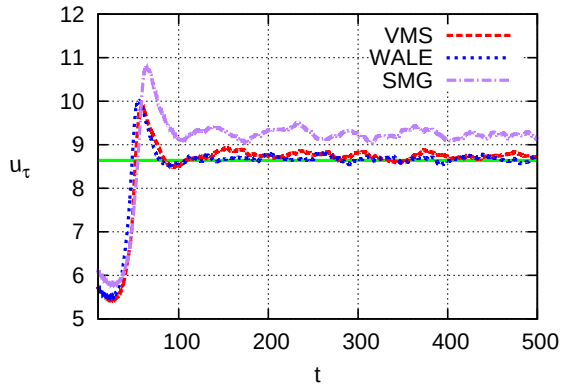

Figure 1. Time evolution of u_τ for the case M03.

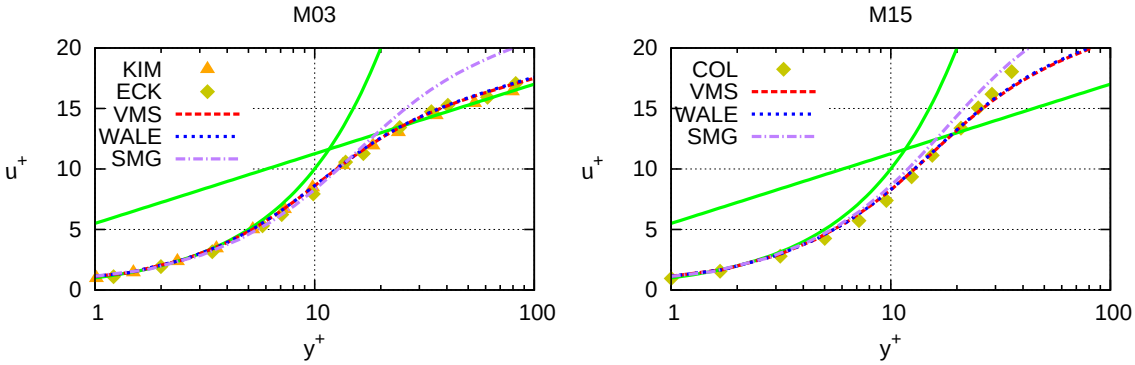

Figure 2. Law of the wall for the case M03 (left) and M15 (right) compared against references. For the inner boundary layer the law $u^+ = 2.5\, ln(y^+) + 5.5$ is used, meanwhile $u^+ = y^+$ is the expression for the outer boundary layer.

Coleman et al. [11] DNS when the WALE or VMS model is used, again the SMG fails in the outer boundary layer. We can see how the logarithmic law rises when the Mach number is increased. Alternative definitions of u^+ can be found in the literature, such as the Van Driest transformation, that accounts for the density variations that causes this difference.

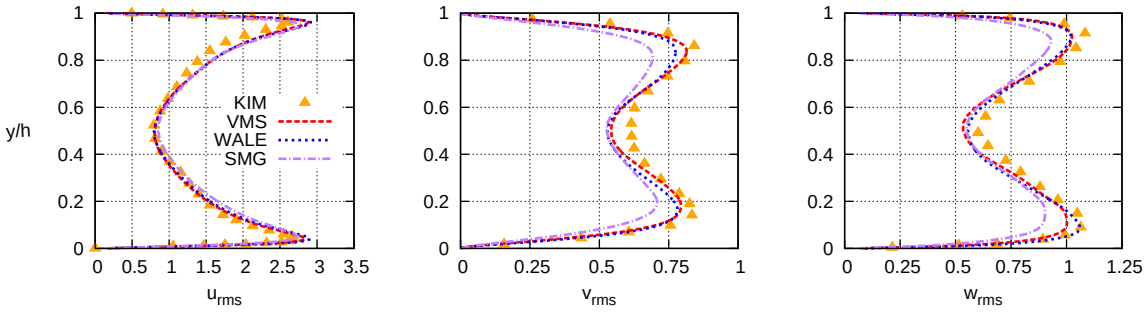

Figure 3. Root-mean-square velocity fluctuations for the case M03, compared to Kim et al.

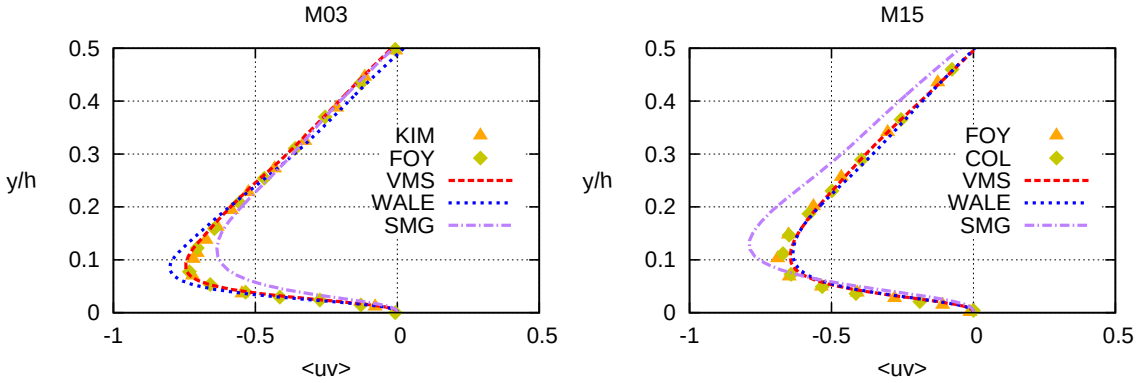

Figure 4. Reynolds shear stresses compared against reference data.

Following with second-order statistics, the root-mean-square velocity fluctuations for the case M03 are presented in figure (3). All three methods give good approximations to reference data, being VMS results slightly better and SMG the worst among the three models. Reynolds shear stresses are depicted in figure (4), showing that for the subsonic case the use of the WALE and SMG models miss-predict the shear stress, due to energy accumulation and over-dissipation, respectively, while the use of VMS match exactly reference DNS. Concerning the supersonic case, both WALE and VMS give fairly good results, being the VMS model slightly better. The use of the SMG model results again in the shear stress over-prediction.

Finally, Q iso-contours of instantaneous fields using the VMS model are presented in figure (5) to evaluate near-wall turbulence structures. It can be seen how near-wall streaks are elongated and more sparsely distributed as Mach number increases.

4. Conclusions & Further Work

Compressible extension of the incompressible LES models implemented in TermoFluids has been carried out. The main differences between the compressible and incompressible formulations are due to the use of a different system of equations (which cause the appearance of extra terms), the isotropic stress tensor (which is null for incompressible flows) and the Favre-averaging. The approximation of the turbulent viscosity is carried out in the same fashion that for the incompressible approach, and no compressible corrections are introduced (also due to the lag of them in the literature).

Concerning the results of the considered SGS models, the WALE and VMS models show

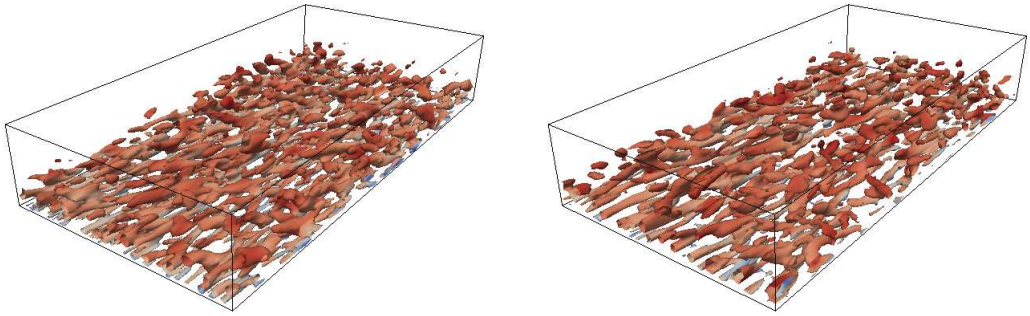

Figure 5. Iso-contours of $Q = 0.1$ colored by Mach number for the case M03 (left) and M15 (right).

good performance on the compressible turbulent channel flow. The SMG model, however, does not perform as good as the other methods. Between the WALE and VMS models, the VMS gives better solutions but results in a more expensive method in terms of computational costs.

The presented results give us confidence to apply the LES models in more complex problems, such as turbulent flows with SBLI. Also, the performance of the models in unstructured meshes and at higher Reynolds is an issue that must be explored. This will be the focus of our future work.

Acknowledgments

This work has been partially granted by the Spanish Secretaría de Estado de Investigación, Desarrollo y Competitividad of the Ministerio de Economía y Competitividad grant for the ENE2014-60577-R project.

References

[1] Lehmkuhl O, Pérez-Segarra C D, Borrell R, Soria M and Oliva A 2007 *Proc. Parallel CFD Conf.* 1–8
[2] Rodríguez I, Lehmkuhl O, Borrell R and Oliva A 2013 *Int. J. Heat Fluid Fl.* **43** 194–203
[3] Lehmkuhl O, Rodríguez I, Bàez A, Oliva A and Pérez-Segarra C D 2013 *Comput. Fluids* **84** 176–89
[4] Lehmkuhl O, Rodríguez I, Borrell R, Chiva J and Oliva A 2013 *Phys. Fluids* **26** 12
[5] Wilcox D 1998 *Turbulence modeling for CFD* (DCW Industries, Inc.)
[6] Catris S and Aupoix B 2000 *Aerosp. Sci. Technol.* **4** 1–11
[7] Pedro J B, Bàez A, Lehmkuhl O, Pérez-Segarra C D and Oliva A 2015 *Proc. Turbulence, Heat and Mass Transfer 8*
[8] Garnier E, Adams N and Sagaut P 1993 *Large Eddy Simulation for Compressible Flows* (Springer)
[9] Sandham N D, Yao Y F and Lawal A A 2003 *Int. J. Numer. Method H.* **24** 584–95
[10] Kim J, Moin P and Moser R 1987 *J. Fluid Mech.* **177** 133–66
[11] Coleman G N, Kim J and Moser R 2004 *J. Fluid Mech.* **305** 159–83
[12] Foysi H, Sarkar S and Friederich R 2004 *J. Fluid Mech.* **509** 207–16
[13] Pino M, Piomelli U and Candler G V 2000 *Theor. Comp. Fluid Dyn.* **13** 361–67
[14] Ducros F, Laporte F, Soulères T, Guinot V, Moinat P and Caruelle B 2000 *J. Comput. Phys.* **161** 114–39
[15] White J A, Baurle R A, Fisher T C, Quinlan J R and Black W S 2012 Low-Dissipation Advection Schemes Designed for Large Eddy Simulations of Hypersonic Propulsion Systems.
[16] Erlebacher G, Hussaini M Y, Speziale C G and Zang T A 1992 *J. Fluid Mech.* **238** 155–85
[17] Nicoud F and Ducros F 1999 *Flow Turbul. Combust.* **62** 183–200
[18] Eckelmann H 1970 Mitteilungen aus dem mpi fr stromungsforschung und der ava. Gottingen